

Possibilities, Limits, and Tradeoffs for Refrigerants in the Vapor Compression Cycle

Mark O. McLinden, PhD

Member ASHRAE

Piotr A. Domanski, PhD

Fellow ASHRAE

Andrei Kazakov, PhD

Jaehyeok Heo, PhD

J. Steven Brown, PhD, PE

Member ASHRAE

ABSTRACT

We explore the possibilities for refrigerants having low global warming potential (GWP) by use of two distinct, but complementary, approaches. In the first approach, we evaluate the effect of a refrigerant's fundamental thermodynamic parameters on its performance in the simple vapor compression cycle and several variations on the basic cycle; this defines the limits of what is thermodynamically possible for a refrigerant. The analysis employs evolutionary algorithms, and it identifies the critical temperature, critical pressure, and ideal-gas heat capacity as the most significant fluid parameters. There is a fundamental tradeoff between high efficiency and high volumetric capacity for the vapor compression cycle. Performance differences between refrigerants in the simple cycle can be reduced by proper cycle modifications. In the second approach, we examine more than 56 000 chemical compounds from a public-domain database of chemical structures. A subset of about 1200 candidate fluids is identified by applying screening criteria to estimates for GWP, flammability, stability, toxicity, and critical temperature. The fluids with critical temperatures below 400 K (i.e., those that could be used in current equipment with minor modifications), are dominated by halogenated olefins. Additional chemical families, including ethers and cyclic compounds, are represented among the fluids having critical temperatures above 400 K.

INTRODUCTION

In the search for new refrigerants having a low global warming potential (GWP), a number of other criteria must also be met. As laid out by McLinden and Didion (1987), these include stability within the refrigeration system and a short atmospheric lifetime (which is related to GWP and ozone depletion potential (ODP)), attributes that are often mutually exclusive. Also important are thermodynamic properties matched to the application, low flammability and toxicity, and other practical considerations, including cost and compatibility with the materials of construction. McLinden and Didion employed thermodynamic arguments and a database search to assess the possibilities for low-ODP refrigerants; the present work is in some ways a reprise of that earlier work, but with the additional constraint of GWP and with the advantage of significantly advanced methods.

M.O. McLinden is a Chemical Engineer and A. Kazakov is a Physicist in the Thermophysical Properties Division, National Institute of Standards and Technology (NIST), Boulder, CO. P.A. Domanski is a Mechanical Engineer and Group Leader and J. Heo is a Guest Researcher in the Energy and Environment Division, NIST, Gaithersburg, MD. J.S. Brown is an Associate Professor in the Department of Mechanical Engineering, The Catholic University of America, Washington, DC. This paper is a contribution of the National Institute of Standards and Technology; it is not subject to copyright in the United States.

The “optimum” refrigerant depends on the constraints of the day, and so the choice of refrigerants must be reconsidered when those constraints change. A major research effort on the part of chemical manufacturers, governments, trade groups, and universities was carried out in the 1990s to identify low-ODP refrigerants. That work (which is well summarized by Bivens and Minor, 1998) resulted in the development of several hydrofluorocarbons (HFCs) that are the dominant refrigerants in use today. Bivens and Minor described investigations into ethers and also compounds based on silicon, sulfur, and nitrogen, but they reported consideration of only fluorinated compounds (chlorine and bromine were considered off limits because of ozone depletion concerns) and make no mention of olefins (compounds with a carbon-carbon double bond). Finding low-ODP refrigerants was the major concern at that time, although Bivens and Minor emphasize the importance of a short atmospheric lifetime, which is important for both ODP and GWP.

The task of identifying new refrigerants can be undertaken in various ways. One approach would be to simulate known fluids to find the best match to the refrigerant currently used in a particular application in terms of coefficient of performance (COP), volumetric capacity, operating pressures, etc. However, the number of fluids with sufficient property data for such a detailed comparison is very limited—on the order of one hundred. In any event, this approach would be, almost by definition, of limited utility in searching for new fluids.

Fluids not presently used as refrigerants could be screened. Many millions of chemical compounds have been reported in the literature, but the vast majority of these compounds would be totally unsuitable for use as a refrigerant (many are solids or are unstable, for example). Furthermore, even the most basic properties that would determine a chemical’s suitability for use as a refrigerant are unknown for most of them. Accurate GWP values, for example, are known for only about 100 compounds. This approach would thus require the extensive application of estimation methods. It is feasible to estimate only the most basic of fluid parameters for a large number of candidates, but before this can be attempted, a coarse filter must be applied to reduce the number of candidates from millions to thousands. But what “coarse filter” is appropriate and what are the optimal values for the fluid properties that can be estimated?

Finally, the thermodynamic behavior of a fluid could be defined in terms of fundamental fluid parameters, such as critical temperature. This allows a simulation of performance (COP, capacity, etc.) in various applications (heating, refrigeration, etc.), and it is not restricted to known refrigerants. Indeed, if a sufficient set of fluid parameters is selected and varied over physically reasonable ranges, nearly the entire universe of refrigerant behavior can be explored. We have termed this the exploration of “thermodynamic space.” This allows the identification of optimal values for fluid parameters for a particular application, but how do these optima relate back to real fluids?

In this work, we combine two of the above approaches. We explore “thermodynamic space” by use of the concept of corresponding states to model the fluid properties; this allows us to simulate fluids in terms of nine parameters. By use of evolutionary algorithms, we identify the most important thermodynamic parameters and their optimum values. In the second approach, we select from a public-domain database of 31 million chemical compounds a set of 56 000 candidate molecules composing only a limited set of elements and having 15 or fewer atoms in the molecule. For these candidates we estimate the GWP, flammability, and critical temperature, and filter out those molecules having functional groups known to be generally toxic or unstable. This yields a set of about 1200 candidate refrigerants. The details of this analysis are presented by Kazakov et al. (2012) and are only summarized here.

APPROACH 1—EXPLORATION OF THERMODYNAMIC SPACE

The requirement for suitable thermodynamic properties is vital. A refrigerant is the working fluid in a thermodynamic cycle and so must possess thermophysical properties that are matched to the cycle that it is used in. A mismatch between the properties and the cycle will result in low efficiency and/or capacity. Domanski et al. (1994) demonstrated that refrigerants can exhibit large performance variations in different modifications of the simple vapor compression cycle; thus, it is important to expand the analysis beyond the baseline cycle. An evaluation of candidate fluids based on thermodynamic properties and cycle simulation studies is an efficient way to proceed—only if a fluid passed this test would it be worthwhile

to consider the lengthy and expensive process of testing toxicity, developing a production process, identifying compatible materials, etc. The lack of property data, however, is a barrier to the consideration of many candidates, and thus a more fundamental approach is called for.

We explore “thermodynamic space” in terms of fundamental fluid parameters, such as critical temperature and vapor heat capacity. By use of evolutionary algorithms, we identify the most important thermodynamic parameters and their optimum values. We use the concept of corresponding states to model the fluid properties; this allows us to simulate fluids in terms of nine property parameters. Thus, this approach is not limited to fluids that are known, although corresponding states calculations are tied to real “reference fluids,” so that thermodynamic consistency between properties is maintained. To date, this type of study has been done in a less systematic way, *e.g.* an analysis of only the ideal vapor compression cycle or using simple cubic equations of state that cannot capture the full range of possible fluid behavior. For example, McLinden (1990) used the principle of corresponding states to determine the optimum T^{crit} and optimum C_p° to find “optimum” refrigerants for several variations on the simple vapor compression cycle for refrigerator applications. Brown (2007) used the Peng-Robinson (P-R) equation of state (EOS) to study known fluids as potential R-114 replacements in high-temperature heat-pumping applications. In addition, he used the P-R EOS to parametrically vary the fundamental thermodynamic parameters T^{crit} , p^{crit} , ω , and C_p° to “design” “ideal refrigerants” for high-temperature heat-pumping applications for two cases: maximum COP and maximum volumetric capacity. Then in a series of papers, Brown and his co-workers evaluated a number of not-so-well-described refrigerants (those with little or no publically available thermodynamic property data) in various applications, including the performance of eight fluorinated propene isomers in heating and cooling applications (see, *e.g.*, Brown 2009). Domanski et al. (1994) simulated known fluids but examined the results in terms of thermodynamic parameters and showed, for example, that fluids with high values of C_p° had generally lower COP, but that this trend was reversed with the addition of a liquid-line/suction-line heat exchanger.

Properties—Extended Corresponding States

For the exploration of “thermodynamic space” to identify the optimum characteristics of refrigerants, we employ the extended corresponding states (ECS) model of Huber and Ely (1994). The principle of corresponding states leads to the result that the reduced Helmholtz energy A of fluid j and a reference fluid (designated by subscript “ref”) are related by

$$\left[\frac{A(T_j, \rho_j) - A^0(T_j, \rho_j)}{RT_j} \right]_j = \left[\frac{A(T_{\text{ref}}, \rho_{\text{ref}}) - A^0(T_{\text{ref}}, \rho_{\text{ref}})}{RT_{\text{ref}}} \right]_{\text{ref}}, \quad (1)$$

where the superscript 0 refers to the ideal-gas state (vapor in the limit of zero pressure) and the reference fluid is evaluated at a temperature and density given by

$$T_{\text{ref}} = T_j / f_j \quad \text{and} \quad \rho_{\text{ref}} = \rho_j h_j. \quad (2, 3)$$

The f_j and h_j are termed “equivalent substance reducing ratios” and are given by

$$f_j = T_j^{\text{crit}} / T_{\text{ref}}^{\text{crit}} \quad \text{and} \quad h_j = \rho_{\text{ref}}^{\text{crit}} / \rho_j^{\text{crit}}, \quad (4, 5)$$

where the superscript crit refers to a critical property of the fluid.

All other thermodynamic properties stem from these relationships. For example, the compressibility factor is given by

$$Z_j(T_j, \rho_j) = \frac{p_j}{RT_j \rho_j} = Z_{\text{ref}}(T_j / f_j, \rho_j h_j). \quad (6)$$

In other words, to calculate the compressibility factor of fluid j , an EOS for the reference fluid is evaluated at some different temperature and density, as given by the ratios of critical parameters defined by Eqs. (2–5).

The equations above describe simple corresponding states. These apply only to spherically symmetric molecules that are conformal, *i.e.*, have the same intermolecular forces on a reduced basis. To *extend* the method to other molecules that may be polar and non-spherical, the equivalent substance reducing ratios f_j and h_j are made to be functions of temperature and density (although only temperature dependence is considered here):

$$f_j = \frac{T_j^{\text{crit}}}{T_0^{\text{crit}}} \theta_j(T, \rho) \quad (7)$$

and

$$h_j = \frac{\rho_0^{\text{crit}}}{\rho_j} \phi_j(T, \rho), \quad (8)$$

where θ_j and ϕ_j are “shape factors” that are fitted to data.

The strength of the ECS approach is its ability to provide a representation of fluid properties with good accuracy given only a limited set of data or, for the present application, to provide thermodynamically consistent properties in terms of a limited number of parameters (in addition to the parameters defining the reference fluid EOS).

Faced with the need in 1994 to calculate the properties of numerous “new” refrigerants having limited data, Huber and Ely developed the following functional forms for the shape factors:

$$\theta_j = 1 + (\omega_j - \omega_{\text{ref}})(\alpha_1 + \alpha_2 \ln T_j^r) \quad (9)$$

and

$$\phi_j = \frac{Z_{\text{ref}}^{\text{crit}}}{Z_j^{\text{crit}}} \left[1 + (\omega_j - \omega_{\text{ref}})(\beta_1 + \beta_2 \ln T_j^r) \right], \quad (10)$$

where the acentric factor ω basically defines the slope of the reduced vapor pressure curve and is defined as

$$\omega_j = -1 - \log_{10} \left(\frac{p_j^{\text{sat}}(T = 0.7 \cdot T_j^{\text{crit}})}{p_j^{\text{crit}}} \right), \quad (11)$$

where p^{sat} is vapor pressure and the reduced temperature is given by

$$T_j^r = \frac{T_j}{T_j^{\text{crit}}}. \quad (12)$$

Huber and Ely fitted the α_1 , α_2 , β_1 , and β_2 parameters to 21 refrigerants using vapor pressure and saturated liquid density data along with experimental values of the critical parameters. R-134a was used as the reference fluid. For our application of exploring “thermodynamic space,” the following parameters are to be optimized:

$T^{\text{crit}}, p^{\text{crit}},$

ω , and

$\alpha_1, \alpha_2, \beta_1$, and β_2 .

The above applies to the “residual” properties, *i.e.*, differences with the ideal-gas state. For a full representation of the thermodynamic properties, the ideal-gas portion of Eq. (1) must also be included. This can be done in terms of the ideal-gas Helmholtz energy \mathcal{A}° , but it is conventionally done in terms of the ideal-gas heat capacity C_p° , which is defined here in terms of its value at the arbitrary temperature of 300 K, $C_p^\circ(300 \text{ K})$; this is further modified by a parameter γ which defines the temperature dependence:

$$C_p^0(T) = C_p^0(300 \text{ K})[1 + \gamma(T - 300)]. \quad (13)$$

For all but the simplest molecules, C_p° can be a complex function of temperature. A simple linear function in temperature is justified in this application because of the limited temperature range over which most refrigeration cycles operate. The NIST REFPROP database (Lemmon et al. 2010), which implements a number of thermodynamic models (including the ECS model) was used for the calculation of refrigerant properties. Note: It can be shown through manipulation of Eqs. (7)-(12) that the ECS formulation is independent of both p^{crit} and Z^{crit} .

Table 1 lists the parameters that were varied in the optimization and their ranges. T^{crit} , p^{crit} , ω , and C_p° are fundamental thermodynamic parameters of a fluid, and the others are fitting parameters for the model used; together they describe the thermodynamic behavior. Two reference fluids were used: propane and R-32. These two fluids are typical of non-polar and polar refrigerants, respectively, and both have very good equations of state that are valid over wide ranges of temperature and pressure—requirements for a reference fluid formulation. Ranges must be specified to constrain the optimization to physically reasonable bounds. The ranges given in Table 1 are based largely on the 105 pure fluids in REFPROP; these compose all of the common refrigerants (both synthetic and natural) as well as additional simple organic and inorganic molecules that have boiling points in the range of current refrigerants. The critical temperature covers the range from near the condenser temperature in the cycles to be investigated here to a temperature near the critical temperature of water. All other parameters span the range of values observed for fluids in REFPROP, with only a few exceptions. Critical pressures lower than 2.0 MPa are observed only for hydrogen, helium, and complex molecules, which are not suitable for a vapor compression cycle at normal refrigeration temperatures. While water has a critical pressure of 22.064 MPa, the upper bound for the current optimization was set to 12 MPa, which is slightly above the next-highest p^{crit} , namely 11.333 MPa for ammonia. This greatly limits the search space for this parameter, a space that is not likely to contain any actual fluids. Negative values of the acentric factor ω are observed only for hydrogen and helium. Values of $C_p^\circ(300\text{ K})$ larger than $300\text{ J}\cdot\text{mol}^{-1}\cdot\text{K}^{-1}$ are observed for heavy hydrocarbons (greater than about C8), but again, these are not suitable for our application.

Cycle Analysis

A modified version of the cycle simulation package CYCLE_D, Version 5 (Brown et al., 2012) was used for the cycle analyses. The cycles considered represent three idealized applications—cooling, refrigeration, and heating—which were characterized by the temperatures in the condenser and evaporator. The evaporator superheat and condenser subcooling were assumed to be zero; the evaporator and the condenser were assumed to have no pressure drop; the refrigerant lines were assumed to have no pressure drop and no heat losses/gains to/from the ambient; and the compressor isentropic efficiency was assumed to be 100%. For each application, four cycle configurations (see Figure 1) were considered: (a) the

Table 1. Fluid parameters varied in the optimization runs, and their ranges and granularity.

Parameter	Units	Range	Granularity
reference fluid	—	propane, R32	
T^{crit}	K	305 ~ 650	0.5
p^{crit}	MPa	2.0 ~ 12.0	0.05
ω	—	0.0 ~ +0.6	0.005
α_1	—	−0.3 ~ +0.3	0.01
α_2	—	−0.8 ~ 0.0	0.1
β_1	—	−1.0 ~ +1.0	0.01
β_2	—	−0.8 ~ +0.8	0.1
$C_p^\circ(300\text{ K})$	$\text{J}\cdot\text{mol}^{-1}\cdot\text{K}^{-1}$	20.8 ~ 300	0.2
γ	K^{-1}	0 ~ 0.0025	0.0001

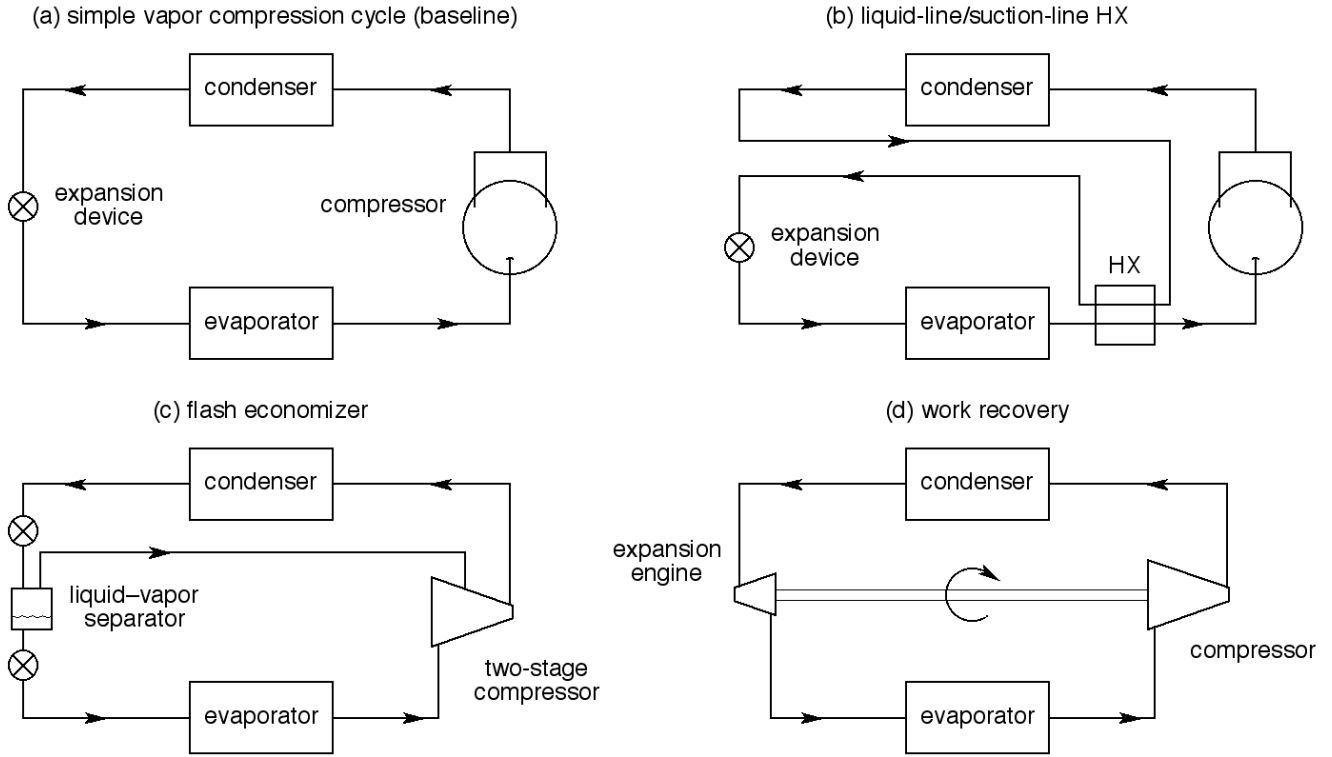


Figure 1. Vapor compression cycles studied in the genetic optimizations: (a) simple (baseline) vapor compression cycle; (b) cycle with liquid-line/suction-line heat exchanger (LLSL-HX effectivenesses of 50% and 100% were considered); (c) economizer cycle with two-stage compression; and (d) cycle with work recovery from expansion device.

simple (baseline) cycle as described above, (b) the baseline cycle with the inclusion of a liquid-line suction-line heat exchanger (LL/SL-HX efficiencies of 50% and 100% were considered), (c) an economizer cycle with two-stage compression, and (d) a cycle replacing the expansion device of the baseline cycle with a work-recovery device of 50% efficiency. These compose the five cycle options considered, as listed in Table 2.

Optimization by Evolutionary Algorithms

While refrigerant selection involves multiple criteria, as discussed in the Introduction, the optimization of refrigerant thermodynamic properties has two primary objectives: the interest is to maximize both the coefficient of performance (COP) and the volumetric capacity (Q_{vol}). The volumetric capacity is defined as the refrigeration capacity per unit of volume of refrigerant vapor flowing into the compressor; it is a measure of equipment size (first cost). COP is an indicator of the energy efficiency (operating cost) of the system. While the merits of high COP and high Q_{vol} could be expressed in monetary terms allowing these two to be expressed by a single objective, doing so would require problematic simplifications and assumptions, which would render the optimization less general. This is evident by considering the fundamental tradeoff that exists between COP and Q_{vol} : for a given cycle, refrigerants with a high COP tend to have a low Q_{vol} , and vice versa. (This is a general trend valid when comparing a large number of refrigerants; in comparing a limited number of fluids it is possible to find refrigerants that have higher COP and Q_{vol} compared to some other fluid.)

In general, the optimization process involves evaluating different candidate solutions from a given domain space and selecting the solution that is the “best one” for the given objectives. Our approach is to apply the principles of genetic optimization, whereby a set of candidate fluids (known as a “population” or “generation”) is simulated in a given cycle and application. The results are used to select “children” (*i.e.*, fluids with a different set of thermodynamic parameters) for the

Table 2. Summary of cycle simulations.

Application	T_{evap} (°C)	T_{cond} (°C)	Cycle option	Upgrade over simple cycle
Cooling	10	40	1	None
			2	LL/SL-HX; 50% effectiveness
			3	LL/SL-HX; 100% effectiveness
			4	Economizer; optimized intermediate pressure
			5	Work recovery device; 50% efficient
Commercial Refrigeration	-20	30	As above	As above
Heating	-10	30	As above	As above

next “generation.” The “best” fluids from each population are retained, and the process is continued for a prescribed number of generations.

Multi-objective optimization (in most cases) does not provide a unique “best” solution satisfying every objective. The search algorithm will encounter, at first, fluids that have both better COP and Q_{vol} than those of the candidates it has evaluated thus far, but at some point it will no longer be possible to improve one objective without accepting lower values for the other. In multi-objective optimization, this fact is described by the term “Pareto optimality”, and the collected tentative solutions are referred to as non-dominated (Goldberg 1989). For our bi-objective problem, this set of non-dominated solutions forms the so-called Pareto front on the COP – Q_{vol} plane, which graphically represents the boundary to what can actually be realized, *i.e.*, the highest possible COP for a given value of Q_{vol} , and vice-versa.

The search domain for this study, termed “thermodynamic space”, is defined by the nine EOS parameters and their ranges presented in Table 1. The table also includes the granularity for each parameter, representing the smallest increment for a parameter deemed to have a significant impact on the solution. Optimization runs were executed by EOS-EVOL, a multi-objective evolutionary optimization tool (Wojtusiak, 2011). EOS-EVOL worked in tandem with CYCLE_D, which evaluated the refrigerant performance. EOS-EVOL generated sets of nine EOS parameters (which characterized the candidate fluids) following its evolutionary scheme and provided these to CYCLE_D, which calculated the COP and Q_{vol} . Upon completion of the optimization run, EOS-EVOL identified the solutions (*i.e.*, sets of fluid parameters) lying on the Pareto front for further “manual” analysis and interpretation.

Details regarding EOS-EVOL are beyond the scope of this paper, and only basic information is provided here. EOS-EVOL combines traditional evolutionary operators with guided machine-learning-based approaches (Wojtusiak and Michalski, 2006). The optimization run starts with a set of randomly generated candidate solutions, which constitute the first population. For each iteration (population), new candidates are created by either machine learning or by applying traditional evolutionary operators. Additionally, a number of new candidate solutions were randomly generated during each iteration. (This was intended to help prevent the optimization from becoming trapped in local minima.) We executed each optimization run using the following main EOS-EVOL control parameters: population size = 100; number of populations = 200; number of children/solutions generated for each population = 25; number of random candidate solutions in each population = 5. Accordingly, each optimization run examined $100 \times 200 = 20\,000$ candidate solutions. To obtain a sufficient number of non-dominated solutions to create a smooth Pareto front, we executed five optimization runs for each cycle option and application condition, which involved a total of 100 000 candidate fluids.

APPROACH 2—SCREENING OF CANDIDATE MOLECULES

We start with the public domain PubChem database of the National Institutes of Health (Bolton et al. 2008), which lists more than 31 million compounds. This number is reduced to a more tractable 56 000 candidates by considering only

molecules with 15 or fewer atoms and comprising only the elements C, H, F, Cl, Br, N, and/or S. Radicals, ions and ionic compounds, and compounds containing specific atomic isotopes were excluded. We limit the maximum molecular size to 15 atoms, because the refrigerants in current commercial use are all small molecules. The largest molecule listed in the ASHRAE (2010a) classification standard for refrigerants, for example, is pentane, with 17 atoms, but this fluid is used primarily as a minor constituent in blends. A study by McLinden (1990) provides a thermodynamic basis for preferring small molecules: the optimum range of critical temperature was $340\text{ K} < T^{\text{crit}} < 470\text{ K}$, with values of the ideal-gas heat capacity in the range $35 < C_p^\circ < 210\text{ J mol}^{-1}\text{ K}^{-1}$ (depending on which variation on the simple vapor-compression cycle was considered). Such values are observed for alkanes with three to five carbons or halogenated alkanes with three or fewer carbons. The choice of elements traces back to Midgley (1937) who observed that only a small portion of the periodic table would form compounds sufficiently volatile to serve as a refrigerant. This is likewise confirmed by the ASHRAE (2010a) standard, where the only exceptions among the listed refrigerants are helium, neon, and argon, which are used in cryogenic refrigeration systems, but which have boiling points and critical temperatures that are too low for normal refrigeration applications. We include chlorine and bromine despite their potential to deplete stratospheric ozone. A compound containing Cl or Br, and having a very short atmospheric lifetime, would have a very small ODP and might be acceptable. For example, the U.S. EPA has approved the use of R-1233zd(E) ($\text{C}_3\text{H}_2\text{ClF}_3$) in chiller applications (U.S. EPA 2012).

The requirement for screening fluids based on their GWP is driven by current and proposed regulations. We selected a target value of $\text{GWP}_{100} < 200$ based on current policy outlook (Mascarelli 2010), including the so-called Mobile Directive of the European Union (2006), which mandates fluids with $\text{GWP}_{100} < 150$ in automotive air conditioning, and a joint United States/Canada/Mexico proposal to the Montreal Protocol (the international treaty regulating ozone-depleting substances) that would phase down the use of HFCs to 15% of 2004–2006 consumption levels by 2033 (U.S. State Department 2009). The ideal refrigerant would be non-flammable, but moderate flammability may be acceptable. We take as “moderate” a lower flammability limit greater than 0.1 kg m^{-3} , which corresponds to the boundary between the “Class 2” and “Class 3” flammability ratings in the ASHRAE (2010a) refrigerant classification standard. We are thus also including refrigerants that would be classified as “2L” (those having burning velocities less than 10 cm s^{-1}).

We use the critical temperature as the primary thermodynamic criterion. The lower bound is 300 K; this is the approximate lowest operating temperature of the condenser in a cycle rejecting heat to ambient air; fluids with lower values of T^{crit} would operate in a supercritical cycle. As the refrigerant T^{crit} increases, the cycle operates at lower reduced temperatures and pressures; this generally results in higher efficiencies (McLinden 1990) but the volumetric capacity Q_{vol} decreases, requiring physically larger equipment. Operation at subatmospheric pressures is problematic because air leakage would be into the sealed system, degrading performance of the heat exchangers and, for flammable refrigerants, creating an explosion hazard. For these reasons, the most commonly used refrigerants have $343\text{ K} < T^{\text{crit}} < 385\text{ K}$. Systems with centrifugal-type compressors often use fluids having higher critical temperatures, up to about 471 K. We adopt 550 K as a generous upper limit on critical temperature, so as not to prematurely exclude otherwise promising candidates.

Safety codes (*e.g.* ASHRAE 2010b) require refrigerants of low toxicity in residential and most commercial applications. A refrigerant is expected to operate many years in a sealed system, so that unstable compounds are not suitable. For these properties, we filter out molecules containing functional groups that are generally expected to be toxic and/or unstable. We emphasize that these are very coarse filters. Fluids passing these filters may be considered class “B” (“more toxic”) under the more stringent criteria of ASHRAE Standard 34 (2010a). Ammonia, for example, was not screened out by these filters.

The estimation methods employed here require the three-dimensional structure of the molecule. Initial three-dimensional molecular structures were produced with an improved and extended version of a procedure previously developed by Kazakov *et al.* (2010), with sampling, where applicable, of multiple conformations and stereoisomers. A final single structure was chosen based on the lowest free energy at standard conditions obtained at the level of theory used. While the 3-D structures were included in the PubChem database for about 20 000 of the compounds considered, Kazakov *et al.* (2012) calculated the structure of all 56 000 to maintain consistency.

Estimation of GWP

The global warming potential (GWP) of a chemical results from the combination of its *radiative forcing* and *atmospheric lifetime*, together with the time frame for evaluation. The radiative forcing is the “change in net irradiance at the tropopause” (Houghton et al. 1996) due to the change in atmospheric concentration of a trace gas resulting from a pulse release of that gas. (The tropopause is the upper boundary of the troposphere and is located 9 to 17 km above the Earth's surface.) The *radiative efficiency* (RE) is the radiative forcing for a unit change in atmospheric concentration; it has units of $\text{W m}^{-2} \text{ppbv}^{-1}$ (where ppbv is volume or molar concentration in parts in 10^9). Taking a global mean for the atmospheric concentration and a simple exponential decay for the time-dependent concentration of the trace gas, the GWP is given by

$$\text{GWP} = \left\{ \frac{\text{RE} \times \tau [1 - \exp(-\text{TH}/\tau)]}{W} \right\} \bigg/ \int_{\tau=0}^{\text{TH}} \frac{\text{RE}_{\text{CO}_2} \times c_{\text{CO}_2}(t)}{W_{\text{CO}_2}} dt, \quad (14)$$

where RE and RE_{CO_2} are radiative efficiencies and W and W_{CO_2} are molar masses of the trace gas and reference gas (CO_2), respectively; τ is the atmospheric lifetime of the trace gas; and $c_{\text{CO}_2}(t)$ is the time-dependent concentration of the reference gas, which is given by a model more complex than a simple exponential decay. TH is the time horizon, and $\text{TH} = 100$ years is used here, which is the most common value referenced in regulations. The determination of GWP requires detailed simulations of atmospheric transport, radiative heat transfer, and multiple removal mechanisms for a trace gas. This has been done for only a small number of compounds, and most of the 100 or so GWP values reported in the literature are based on Eq. (14) along with separately estimated values of RE and τ .

The concept of GWP has a number of weaknesses. Eq. (14) considers only the direct effects of the emission of a trace gas. The reaction products resulting from atmospheric breakdown of the trace gas have radiative efficiencies and lifetimes of their own. The second major issue of concern, especially in the present context, is that the assumption of a global mean concentration breaks down for gases with short atmospheric lifetimes. In such cases, the GWP depends on the emission scenario (location, time of year, etc.), and the GWP given by Eq. (14) represents an upper bound on the actual value.

Given the present objective of screening a large number of compounds, detailed simulations are out of the question, and compromises are necessary. Indirect effects are neglected, and the global-mean approximation is adopted, even for short-lived compounds. A direct estimation of the GWP is not possible for two reasons. First, GWP is a complex characteristic of a chemical and, second, the “learning set” that would be available to develop a direct estimate is very limited and is heavily biased towards present classes of fluids, such as the CFCs, HCFCs, and HFCs. Instead, Kazakov et al. (2012) separately estimated the RE and atmospheric lifetimes of the 56 000 compounds.

A number of methods to estimate RE are available in the literature, and Kazakov et al. (2012) selected the method of Pinnock et al (1995) because it is computationally efficient, applicable to a wide variety of compounds, and exhibits good performance in comparison with more detailed methods. The Pinnock method requires the infrared (IR) absorbance spectrum of the molecule in question, and this was estimated by semiempirical quantum chemical methods. Kazakov et al. (2012) describe extensive testing and comparison of various methods to a “validation set” of about 100 values of RE reported in the literature. In the end, they used IR spectra calculated with the PM6 semiempirical method. The resulting logarithmic root-mean-squared deviation (RMSD) for RE was 1.84, which is reasonable for screening purposes.

The atmospheric lifetime is dependent on multiple removal mechanisms, including ultraviolet (UV) photolysis, rainout, and chemical reaction with hydroxyl radical (OH), ozone, NO_3 , and Cl in the troposphere and, in the stratosphere, by UV photolysis and reaction with OH, ozone, and singlet oxygen. Kazakov et al. (2012) considered only reaction with OH, because this is the dominant loss mechanism for most of the compounds with lifetimes on the order of the considered time horizon of 100 years or less. The reaction with OH is expressed in terms of the first-order rate constant k_{OH} . Techniques for estimating k_{OH} range from group-contribution methods, to correlations based on quantum chemical calculations (e.g., the method of Klamt (1993), known as the MOOH method), to very detailed methods based on *ab initio*

(first principles) calculations. Kazakov et al. (2012) used the group contribution method of Kwok and Atkinson (1995) in an extended implementation (U.S. EPA 2010); this method is slightly less accurate than the MOOH method, but it is applicable to a wider number of compounds. Given an estimate for k_{OH} , the atmospheric lifetime is

$$\tau = \frac{a}{k_{\text{OH}}[\text{OH}]}, \quad (15)$$

where $[\text{OH}]$ is the annual global average concentration of 1×10^6 molecules cm^{-3} (Montzka 2000), and a is an empirical parameter that corrects for various uncertainties in the estimation procedure. The parameter a was determined by fitting estimated and reported lifetimes and was found to be 2.1.

Having estimated values of RE and τ , Kazakov et al. (2012) then determined estimates for GWP_{100} using Eq. 14. The estimated values are compared with the available literature values (which number 103) in Figure 2. The most significant outlier is CF_3I ; the C–I bond is very weak and undergoes very rapid UV photolysis, but this mechanism was not considered in the estimation of lifetime. The reaction rate for CF_3I with OH is slow, and the estimation method predicts a very long lifetime. Overall, there is significant scatter, but the estimated values follow the expected trend, and the logarithmic RMSD corresponds to a factor of 3.0. This is quite reasonable for screening purposes, especially in view of GWP_{100} ranging over four orders of magnitude.

Estimation of Flammability

Various methods are available for the estimation of flammability, as summarized by Vidal et al. (2004). Again, computational speed and scope of coverage take precedence over achieving the very highest accuracy. Kazakov et al. (2012) started with the correlation between the heat of combustion (ΔH_{comb}) and the lower flammability limit (LFL), with both expressed on a mass basis. The heat of combustion is readily calculated given the heats of formation (see, for example, ASHRAE 2010a, which also gives the combustion products for halogenated materials). The heats of formation for each of the 56 000 compounds were already estimated in the course of determining the IR spectra needed for the RE calculation. To verify the method, heats of combustion for 468 chemicals were calculated by the same methods and compared to experimental values of LFL taken from the DIPPR (2011) compilation, as shown in Figure 3. Although several outliers are present (including hydrogen sulfide and carbon disulfide), the estimation method is generally seen to work well, with a logarithmic RMSD corresponding to a factor of 1.24. These results are correlated by the empirical function

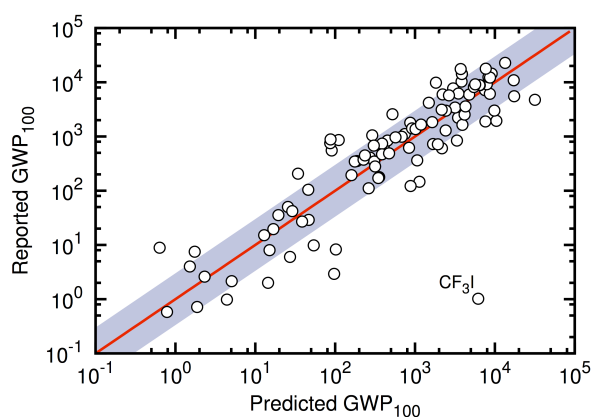


Figure 2. Comparison of estimated and reported GWP_{100} ; the shaded area represents the logarithmic RMSD.

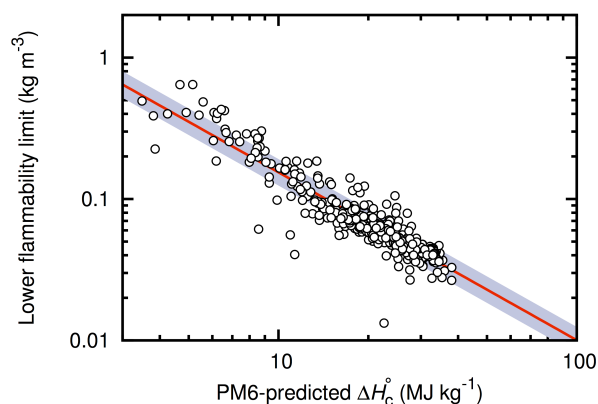


Figure 3. Experimental lower flammability limit versus estimated heat of combustion for 468 chemical compounds.

$$\text{LFL}/\text{kg} \cdot \text{m}^{-3} = 2.38 \times \left(\Delta H_{\text{comb}} / \text{MJ} \cdot \text{kg}^{-3} \right)^{-1.19}. \quad (16)$$

Note that this method and Eq. 16 apply only to materials with a positive heat of combustion. Materials with ΔH_{comb} lower than about $3 \text{ MJ} \cdot \text{kg}^{-3}$ (including negative values) are nonflammable.

Estimation of Critical Temperature and Other Screening Criteria

The estimation of critical temperature and critical pressure are described by Kazakov et al. (2010). The ideal-gas heat capacity C_p° was estimated from a standard statistical-mechanical, rigid-rotor/harmonic oscillator model (McQuarrie 1976). This model required only the vibrational frequencies, and they were taken from the PM6 calculations (which were already done for the RE estimation). A frequency scaling factor of 1.061 (Fekete et al. 2007) was applied.

A cursory toxicity filtering was performed based on a list of markers and associated rules for the elimination of compounds that contain them, compiled by Lagorce et al. (2008). Although this test is by no means comprehensive, it allows elimination of some obviously toxic compounds, and could be performed very rapidly.

An additional screening was applied to eliminate unstable fluids. Compounds with any of the following functional groups were eliminated: (1) triple bond, (2) nitro ($-\text{NO}_2$) group, (3) peroxide ($-\text{O}-\text{O}-$) group, (4) 3- and 4-member rings, (5) disulfide ($-\text{S}-\text{S}-$) group, (6) $-\text{C}=\text{S}$ group, (7) linear diene ($-\text{C}=\text{C}-\text{C}=\text{C}-$), (8) NO and NN groups (any bond order), (9) N-X and O-X groups, where X = F, Cl, or Br, (10) $=\text{C}=$ group, and (11) groups exhibiting keto-enol tautomerism.

RESULTS

Results—Exploration of Thermodynamic Space

The evolutionary optimization of COP and \mathcal{Q}_{vol} was conducted for three typical applications (cooling, heating, and refrigeration) combined with five vapor-compression-cycle options, together with two reference fluids (R-32 and propane) for the ECS model, for a total of 30 optimizations. Approximately 1 million sets of thermodynamic parameters representing hypothetical fluids were simulated for each application. The results were qualitatively similar for the three applications and two reference fluids, so we will discuss in detail here only the results for the cooling case with R-32 as the reference fluid.

The goal of the optimization was to answer two fundamental questions:

- What are the thermodynamic limits for COP and \mathcal{Q}_{vol} in a vapor compression cycle?
- What thermodynamic parameters are most influential in bringing the refrigerant performance to those limits?

Figure 4 presents the optimization results for four cycle options: the simple cycle, the cycle with a 100% effective LL/SL heat exchanger, the economizer cycle, and the cycle with 50% efficient work recovery from the expansion process. For clarity, only those points defining the Pareto front are plotted. (Following the convention in such optimizations, the inverse of COP and \mathcal{Q}_{vol} are plotted, so that solutions satisfying both objectives reasonably well lie at the lower left corner.) For comparison, the figure includes selected refrigerants in current use. Several observations can be made. First, the evolutionary optimizations yield distinct Pareto fronts, suggesting that the starting populations, number of generations, and other parameters of the optimization process were appropriate. Second, as expected, there is a clear tradeoff between COP and \mathcal{Q}_{vol} . And (third), the variation in COP has a total span of only about 20% compared to a variation in \mathcal{Q}_{vol} of over two orders of magnitude.

The Pareto front displays asymptotic behavior for both COP and \mathcal{Q}_{vol} ; *i.e.*, it shows the upper limit of COP or \mathcal{Q}_{vol} that can be obtained if one is willing to accept a low value for the other parameter. (It is interesting to compare the asymptotic COP of $1/0.1105 = 9.05$ from the Pareto front with the Carnot limit of 10.13 (which would be just off-scale on Figure 4) for the condenser and evaporator temperatures simulated here.) The Pareto front for the simple cycle is located farthest from each axis indicating the poorest performance among the various cycle options studied. The character of the Pareto fronts for the economizer cycle and the cycle with work recovery show similar behavior. The cycle with a LL/SL

heat exchanger shows a lower Q_{vol} limit than for the previous two cycle options and a higher COP limit; however, one must bear in mind that this option assumed an idealized 100% effective LL/SL heat exchanger, which is not attainable in practice. Different ranges (lengths) of the Pareto fronts on the charts result from convergence issues in property calculations for the hypothetical fluids when stressed to their thermodynamic limits.

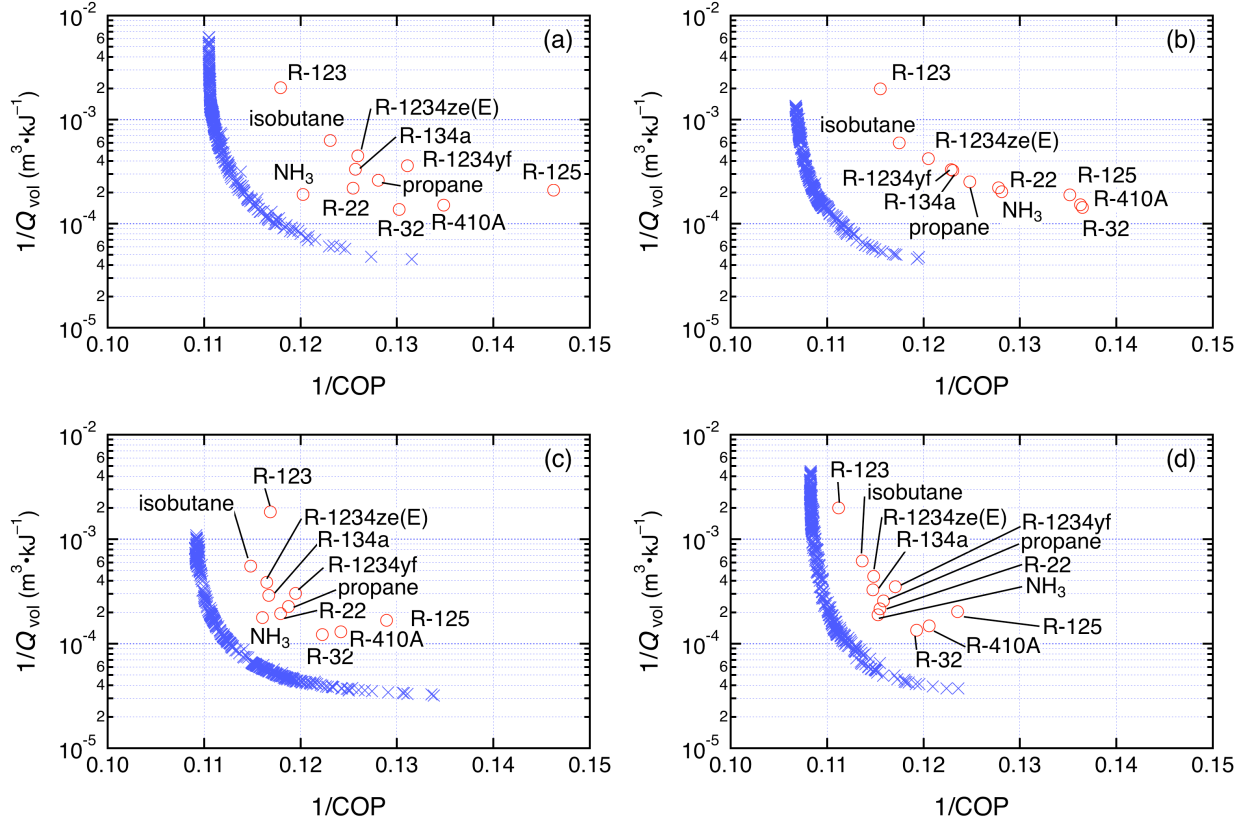


Figure 4. Pareto front (x) and select current refrigerants (o) for the different cycle options: (a) simple vapor compression cycle; (b) cycle with 100% effective LL/SL heat exchanger; (c) economizer cycle; and (d) cycle with 50% efficient work recovery.

As expected, the currently used refrigerants are located well away from the Pareto front for every cycle configuration. This indicates that refrigerants with better performance are, at least, *allowed* by thermodynamics. The relative location of these refrigerants on the different charts is indicative of the influence that different cycle modifications have on the individual refrigerant performance. The observed differences in COPs (between charts) are much larger than those for the Q_{vol} values. The currently used refrigerants are most widely scattered on the basic cycle chart (Figure 4a), and are most tightly grouped for the cycle with work recovery. The work-recovery device improved COP for every fluid; however, it provided a larger COP improvement for poor performers than for better-performing fluids. The economizer also improved COP for every refrigerant but to a smaller degree than for the work recovery cycle. The cycle with the LL/SL heat exchanger provided a mixed influence depending on the molar heat capacity of the refrigerant (Domanski et al., 1994). For example, compared to the simple cycle, the COPs for propane and R-125 (large heat capacities) improved in the cycle with the LL/SL heat exchanger, while the COPs for ammonia (NH_3) and R-32 (small heat capacities) decreased. It is interesting to note that the performance of R1234yf (a HFO of considerable industry interest) is substantially improved by the addition of a LL/SL heat exchanger. (This has been experimentally investigated by Seybold et al., 2011.)

Figure 5 presents a distribution of EOS parameters for the refrigerants forming the Pareto front for the simple cycle. Each set of vertically aligned symbols represents one set of EOS parameters for a given hypothetical refrigerant. Separate

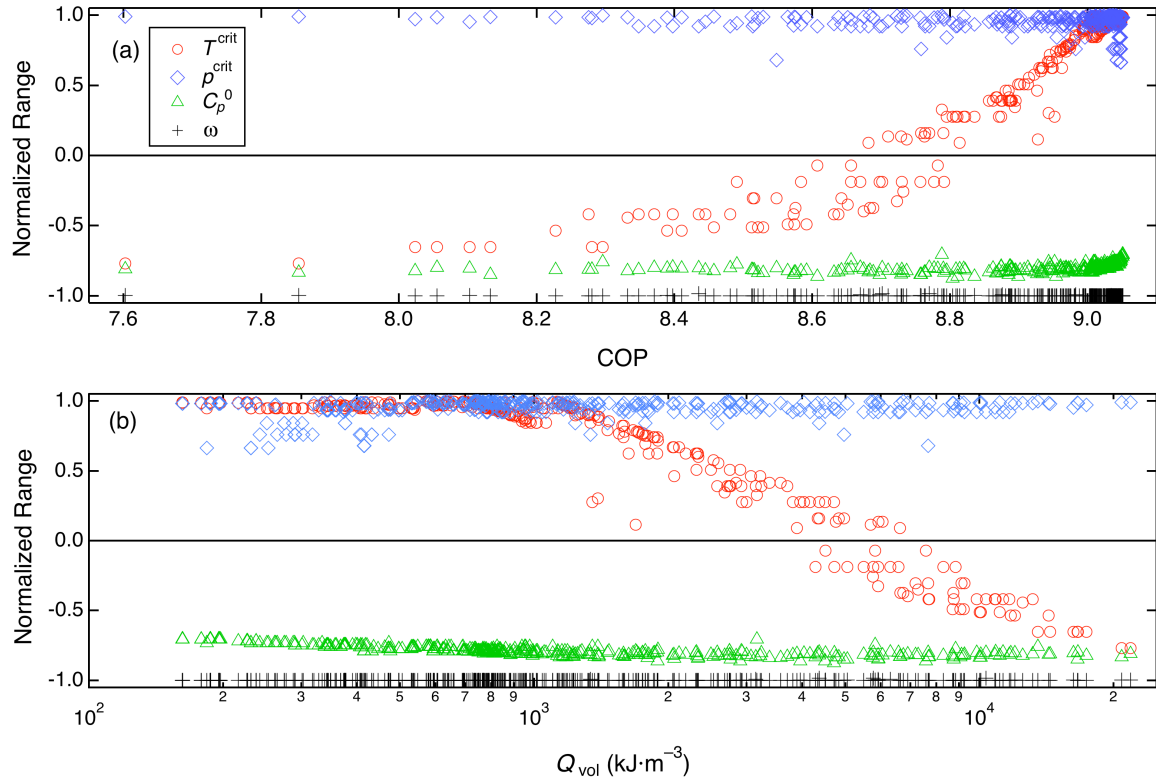


Figure 5. Refrigerant parameters (normalized by the ranges defined in Table 1) for fluids on the Pareto front for the simple vapor compression cycle: (a) ordered by COP and (b) ordered by volumetric capacity.

charts with the refrigerants arranged in order of increasing COP and Q_{vol} are provided. The scale for the vertical axis normalizes the value of each parameter by its range given in Table 1; for example, normalized values of -1 and $+1$ represent T^{crit} values of 305 K and 605 K, respectively. Reviewing the COP chart (Figure 5a), one can see a strong positive dependence of COP on the refrigerant critical temperature; it is the strongest trend shown on the chart. Three other parameters shown on the chart maintain nearly constant values: the values for p^{crit} lie at the very top of its range, except that they drop somewhat for the highest obtained COPs. The values of ω are at the very bottom, and C_p^0 is about 10% above the bottom of its range. Although not shown on the chart for clarity, β_1 lies at the top of the range, and α_2 is at the bottom. The values of γ , α_1 , and β_2 show large scatter, and this indicates an insignificant influence of these parameters. The Q_{vol} chart (Figure 5b), presents the same data sets as those in the COP chart except that they are sorted and displayed in order of increasing volumetric capacity. Thus to some degree, the Q_{vol} chart is a mirror reflection of the COP chart, which is consistent with the COP versus Q_{vol} tradeoff demonstrated by the Pareto front.

The optimal values of the key thermodynamic parameters for the economizer cycle and the cycle with work recovery are very similar to those identified for the simple cycle. The reason is that the simple cycle and economizer cycle have the same “outline” on a thermodynamic diagram. The work recovery cycle differs only in that the expansion process follows a path intermediate between a constant-enthalpy process and a constant-entropy process, compared to the constant enthalpy process of the throttle valve in the simple cycle. A somewhat different distribution was obtained for the cycle with LL/SL heat exchanger. This cycle has an additional process of heat exchange between the compressor suction vapor and subcooled liquid in the liquid line, and this shifts the optimal value of vapor heat capacity to the upper limit of its range ($C_p^0 \sim 300 \text{ J mol}^{-1} \text{ K}^{-1}$). The optimal values of α_1 were distributed within the top 25% of the range, as opposed to being seemingly randomly distributed over the whole range, as was the case for the simple cycle.

Results—Screening of Candidate Molecules

The results of the estimation of GWP for the 56 000 compounds are presented in Figure 6, plotted here on logarithmic coordinates of \tilde{c} (a quantity related to lifetime) versus RE/W (the radiative efficiency divided by the molar mass). On these coordinates GWP₁₀₀ contours are straight lines. A somewhat surprising observation is immediately apparent: the overwhelming majority of compounds have low GWP values, with 93.5% of the 56 000 compounds having GWP₁₀₀ < 200. With few exceptions, the radiative efficiency of the compounds varies over about a single order of magnitude, while the atmospheric lifetime varies over more than four orders of magnitude. In other words, GWP₁₀₀ is controlled mainly by variations in atmospheric lifetime. High reactivity towards OH is thus seen to be the norm, but this reactivity is often associated with many undesirable properties, including toxicity, tendency to polymerize, lack of thermal stability, and incompatibility with materials.

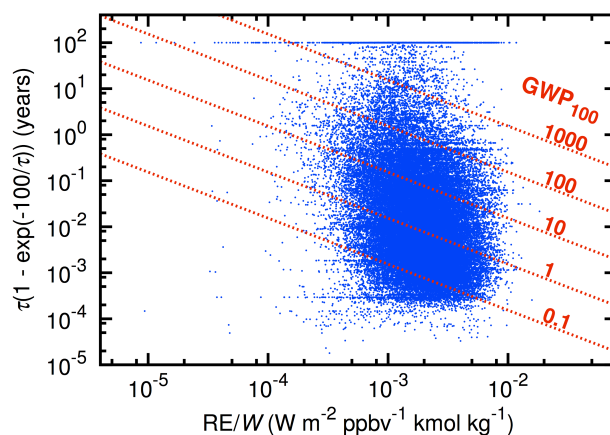


Figure 6. Estimated GWP₁₀₀ for the set of 56 000 compounds.

Among the compounds with the lowest values of GWP₁₀₀ there are two main groups. The diatomic molecules assembled from the elements considered (N₂, O₂, HF, F₂, etc.) have effectively zero values of RE and, thus, zero values of GWP₁₀₀. (These are not shown in Figure 6 because of the logarithmic scaling.) Air components, such as N₂ and O₂, are clearly superior from the environmental point of view, but they are not suitable refrigerants for the vapor compression cycle, because of their low critical temperature. While some of the halogenated diatomics (*e.g.* HF, Cl₂) have boiling points in the range of current refrigerants, they have obvious toxicity and compatibility problems. The second group of very-low-GWP compounds (those towards the lower left corner of Figure 6) include cyclic molecules with multiple sulfur atoms; these include tetrasulfur (S₄) and hexathiene (S₆). These possess a combination of properties that yield very low GWP: the presence of multiple, connected sulfur atoms moves their IR absorption spectra outside the atmospheric window, and they also have very high reaction rates with OH. However, they are not practical as refrigerants because of high melting temperatures and thermal instability.

Thus, a screening based solely on GWP₁₀₀ does not provide a sufficient constraint for selecting candidate refrigerants. Filtering based on other properties is required to obtain a pool of potentially suitable candidates. The filtering criteria (as described above) and corresponding decrease in the number of candidate compounds are presented in Table 3. The toxicity screening, although cursory, does eliminate obviously toxic compounds (such as cyanide compounds). The flammability filter eliminates almost 10 000 additional compounds, even allowing for “moderate” flammability. This filter screened out all of the unsubstituted hydrocarbons, alcohols, and ethers as well as most compounds with a low degree of halogenation. The critical temperature constraint eliminated the compounds that would have very low vapor densities and operating

Table 3. Filtering criteria and resulting count of candidate compounds.

Step	Filter Applied	Constraint	Resulting Count
0	—	—	56 203
1	GWP ₁₀₀	GWP ₁₀₀ < 200	52 565
2	toxicity	see text	30 135
3	flammability	LFL > 0.1 kg·m ⁻³	20 277
4	critical temperature	300 K < T^{crit} < 550 K	1 728
5	stability	see text	1 234

pressures in refrigeration equipment. In many cases, these high- T^{crit} compounds would be solids at the temperatures of interest. The final filter for stability results in about 1200 candidates.

The resulting list of 1200 candidates is finally of a manageable size and contains some number of compounds that would actually be suitable for use as a refrigerant. (The full list is presented in the Supporting Information of Kazakov et al. 2012.) To facilitate the discussion, the candidates are divided into chemical classes, and the results are presented on T^{crit} –GWP₁₀₀ coordinates in Figure 7. The vast majority of the candidates are halogenated because of the flammability constraint. Of the 1200 compounds, only six did not contain one or more halogens. Over 60% of the halogenated candidates contain only fluorine because the addition of heavier chlorine or bromine atoms, while also suppressing flammability, generally results in large increases in the critical temperature, often exceeding the constraint on T^{crit} .

The first group, presented in Figure 7a, are the halogenated alkanes; these are compounds with only single bonds (*i.e.*, they are “saturated”) and comprising only carbon and hydrogen and the halogens fluorine, chlorine, and/or bromine. This class is further divided into linear and cyclic compounds. The linear alkanes (a group which includes the HFCs) generally exhibit relatively high GWP₁₀₀ and high T^{crit} and occupy the upper right corner of the plot. This is the result of competing constraints applied during the filtering. Starting with a hydrocarbon, the critical temperature increases with increased fluorine substitution and reaches a maximum when about one-half of the hydrogens are replaced with fluorine, and then decreases. Reactivity with OH, and thus shorter atmospheric lifetime and lower GWP₁₀₀, is achieved by an increased number of hydrogens. But HFCs with a high hydrogen/fluorine ratio are flammable. Thus, low GWP₁₀₀ favors a high H/F ratio, while low flammability favors a low H/F ratio. The result is that only HFCs with H/F ratios close to 1 pass both the GWP₁₀₀ and flammability filters, and these are compounds with relatively high critical temperatures. The same general trends are also observed for the other halogens. The cyclic alkanes and aromatics are represented by halogenated derivatives of toluene, benzene, and cyclopentane. They have, on average, slightly lower GWP₁₀₀ and higher critical temperatures as compared to the linear alkanes.

The halogenated derivatives of linear olefins are presented in Figure 7b; these are compounds possessing a carbon-carbon double bond (*i.e.*, “unsaturated”) and include the HFOs and HCFOs. They are the largest group among the potential candidates—over a third of the entire set, including a majority of the candidates with $T^{\text{crit}} < 400$ K. The same maximum in critical temperature is observed for hydrogen/halogen ratios near 1, but for the olefins, the dominant mechanism for reaction with OH is addition to the double bond, rather than H-abstraction (as observed for the alkanes). The GWP₁₀₀ for the olefins is thus little affected by the hydrogen/halogen ratio, and compounds possessing the full range of critical temperatures pass both the flammability and the GWP₁₀₀ filters. Cyclic olefins are also represented among the 1200 candidates; because of the stability constraint, which eliminated three- and four-member rings, these are all derivatives of cyclopentene and have $T^{\text{crit}} > 425$ K.

The halogenated oxygenates are plotted in Figure 7c. The linear ethers (compounds possessing a –O– functional group) are the most abundant, covering a wide range of GWP₁₀₀ and critical temperature, including ten with $T^{\text{crit}} < 400$ K.

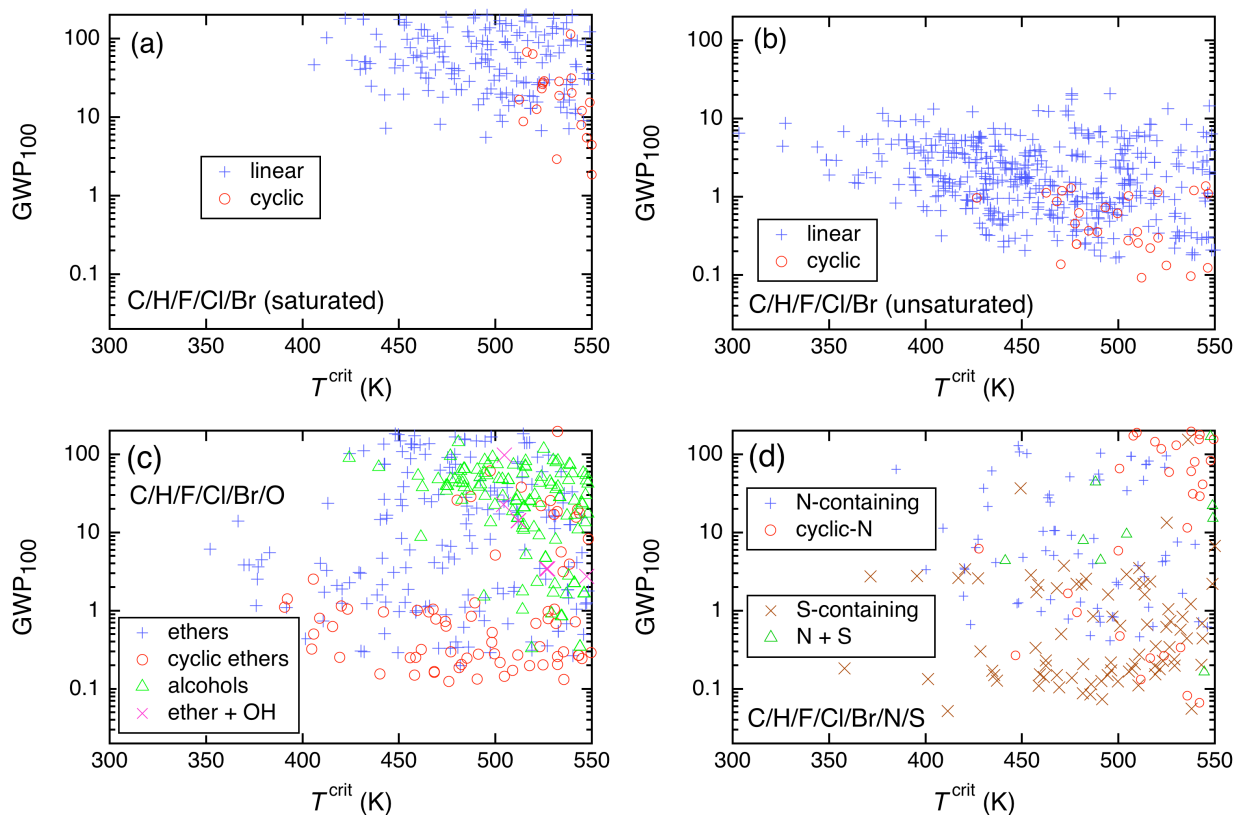


Figure 7. Compounds remaining after applying all filters and grouped by chemical class: (a) alkanes; (b) olefins; (c) oxygenates; (d) compounds containing N and/or S.

However, all of the low T_{crit} ethers also possess a double bond and are thus effectively olefins. The OH reaction rates for C-H sites adjacent to the oxygen are higher than those in alkanes (as reflected by the factors in the method of Kwok and Atkinson 1995) but not substantially higher, so that, as a class, the fluorinated ethers (without double bonds) have GWP_{100} of the same magnitude as the HFCs. The lowest T_{crit} for a linear ether without a double bond is 413 K for $\text{CF}_3\text{OCH}_2\text{CH}_3$, compared to $T_{\text{crit}} = 352$ K for $\text{CF}_3\text{OCF}=\text{CF}_2$, for example. Many of the cyclic ethers also possess a double bond. The halogenated alcohols (compounds with an $-\text{OH}$ group) tend to have high critical temperatures and relatively high GWP_{100} . The lowest T_{crit} among the alcohols is 424 K for CF_3OH . Three compounds have both $-\text{O}-$ and $-\text{OH}$ groups and have critical temperatures above 500 K.

Finally, Figure 7d presents compounds that contain nitrogen and/or sulfur. This group contains the six candidates that have no halogens in the molecule, although all of these have critical temperatures in excess of 470 K. Apart from ammonia (NH_3), which is a very important refrigerant in industrial systems, none of the common refrigerants contain N or S, although these “heteroatoms” offer another alternative to achieve short atmospheric lifetimes and low GWP_{100} . Reaction rates of OH with N and, especially, S are very high. Included here are compounds containing N (either linear, cyclic, or aromatic), containing S, and containing both N and S. Nitrogen compounds in a linear configuration are most prevalent and include mostly amines (derivatives of ammonia, *i.e.*, compounds with three groups attached to a central nitrogen); two with $T_{\text{crit}} < 400$ K are $\text{N}(\text{CF}_3)_2(\text{CF}=\text{CF}_2)$ and $\text{N}(\text{CF}_3)_2(\text{CF}_2\text{H})$. It is interesting to note that Bivens and Minor (1998) discussed 15 fluorinated amines that were studied in the 1990s. Sulfur-containing compounds comprise thiols ($-\text{SH}$, also known as mercaptans) and thiol ethers ($-\text{S}-$). The three compounds with $T_{\text{crit}} < 400$ K are fully fluorinated: CF_3SH , CF_3SCF_3 , and $\text{CF}_3\text{SCF}_2\text{CF}_3$. It should be noted, however, that compounds with N or S are often viewed as problematic due to materials

compatibility concerns (amines and thiols are generally corrosive) or other issues, such as odor in the case of thiols (*tert*-butylthiol is the most common odorant in natural gas, for example).

DISCUSSION

The exploration of “thermodynamic space” has identified optimal values of several key thermodynamic parameters that describe a refrigerant. A screening of 56 000 chemical compounds has revealed about 1200 that might be suitable for use as a refrigerant (or, at the very least, cannot be immediately ruled out) based on their favorable GWP₁₀₀, lack of obvious toxicity, moderate or lower flammability, and suitable critical temperature. Combining the results of these two approaches yields further insights into possible candidates.

The thermodynamic analysis revealed a fundamental tradeoff between efficiency (COP) and volumetric capacity (a quantity that is related to equipment size): refrigerants with higher values of T^{crit} operate further away from the critical point and have higher COP, but also operate at lower pressures (implying larger volumes of vapor that must be compressed). Apart from this tradeoff, which is largely dependent on T^{crit} , the optimum value of the critical pressure was, for the *simple vapor compression cycle*, consistently near the upper limit considered ($p^{\text{crit}} \sim 12$ MPa), and the optimum value of the ideal-gas heat capacity was near the lower limit for this parameter ($C_p^\circ \sim 50$ J mol⁻¹ K⁻¹). The estimated values of p^{crit} and C_p° observed for the 1200 candidates are shown in Figure 8. Unfortunately, the combination of high p^{crit} and low C_p° is very sparsely populated by actual fluids. Only 69 of the 1200 fluids have $p^{\text{crit}} > 5$ MPa, and, of these, only five also have critical temperatures less than 400 K. A number of current refrigerants are also plotted for comparison; ammonia is notable for its unique combination of high p^{crit} and low C_p° .

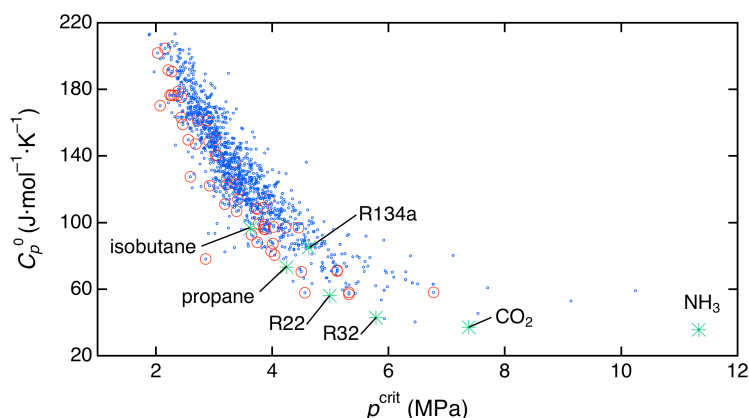


Figure 8. Ideal-gas heat capacity versus critical pressure for the 1200 candidates; those with $T^{\text{crit}} \leq 400$ K are highlighted with a red circle.

The implications of the thermodynamic analysis for refrigerant selection are as follows: Select a refrigerant with a critical temperature based on the economic tradeoff between first costs and operating costs that is appropriate for the application. Select a refrigerant with as high a value of critical pressure as possible given the other constraints. The C_p° should be low for the simple vapor compression cycle or high for a cycle with liquid line/suction line heat exchange. Or, conversely, this last point can be interpreted as: implement a LL/SL heat exchanger (or other cycle modifications) as appropriate to match the thermodynamic characteristics of the refrigerant.

The present set of 1200 candidates was the result of the screening criteria applied, which is to say, our interpretation of acceptable ranges of often competing criteria. We applied toxicity and flammability filters early in the screening process on the assumption that a refrigerant of low toxicity and low-to-moderate flammability (*i.e.*, one which would be classified as A1, A2, or A2L under the ASHRAE (2010a) standard) would be desirable. If one is willing to accept (and the safety codes would allow) use of a refrigerant with a class “B” toxicity rating, then ammonia is an option with excellent thermodynamic characteristics, zero ODP, and a very low GWP. Note that ammonia was the “current” refrigerant lying closest to the

Pareto front in Figure 4a. Likewise, among flammable fluids (those with a class “3” rating), a number of excellent refrigerants are well known and readily available, namely the simple hydrocarbons, such as propane and isobutane, as well as dimethyl ether. It was the task of finding more-or-less direct replacements for the A1-classified HFCs, such as R-134a, that motivated the present work.

The present project is ongoing and future tasks will include more detailed examination of the thermodynamic properties of the 1200 candidate fluids *vis a vis* the optimal parameters identified in the cycle analysis. It is important to note that our screening was based on estimated properties. In particular, fluids passing the toxicity filter may be considered class “B” (“more toxic”) under the more stringent criteria of ASHRAE Standard 34 (2010a). A subset of a few dozen compounds will be selected and studied in more detail, including the effects of the transport properties.

SUMMARY AND CONCLUSIONS

A method for the estimation of global warming potential for a time horizon of 100 years (GWP_{100}) has been developed and validated against literature data. When applied to a library of over 56 000 compounds (considering only molecules with 15 or fewer atoms and comprising only the elements C, H, F, Cl, Br, N, and/or S), we found that screening on GWP alone did not reduce the pool of candidate new refrigerants to a reasonable size, and additional filtering criteria were needed. When additional filters based on toxicity, flammability, stability, and critical temperature were applied, the number of remaining candidates was reduced to about 1200. The fluids with critical temperatures below 400 K (*i.e.*, those that could be used in current equipment with minor modifications) numbered 62, and were dominated by halogenated olefins. Additional chemical families, including ethers and cyclic compounds, are represented among the fluids having critical temperatures above 400 K. The vast majority of the candidates are halogenated; all of the hydrocarbons, as well as the unsubstituted ethers, were filtered out by the flammability criteria.

The exploration of thermodynamic space carried out here outlined the upper performance limit for refrigerants in different vapor compression cycles in terms of COP and volumetric capacity and identified optimum values of thermodynamic parameters required to reach those limits. This information can be helpful in preliminary screening of refrigerant candidates, which should be followed by theoretical cycle simulations employing a complete representation of the thermodynamic processes. When a complete set of thermophysical properties is available, more advanced semi-theoretical cycle simulations that could also account for processes in heat exchangers (affected by conductivity, viscosity and relationship between saturation temperature and pressure) will be most informative regarding the performance of considered refrigerants.

The present analysis is consistent with the current industry interest in the halogenated olefins (*i.e.*, HFOs and HCFOs) as low-GWP refrigerants. These molecules are more complex than the HFCs that they are intended to replace and have different thermodynamic characteristics, such as higher values of C_p° . In contrast to many current studies that compare these new refrigerants with traditional refrigerants in existing equipment, it is clear that modifications to the simple vapor compression cycle will be needed to maximize efficiency.

ACKNOWLEDGMENTS

This work was supported by the U.S. Department of Energy, Office of Energy Efficiency and Renewable Energy under contract no. DE-EE002057 with A. Bouza and B. Habibzadeh serving as Project Managers. We also thank our collaborators J. Wojtusiak of George Mason University, Fairfax, VA, and J. Filliben and A. Pintar of the NIST Statistical Engineering Division.

NOMENCLATURE

a	=	empirical parameter in Eq. 15	c	=	concentration
A	=	Helmholtz free energy	\tilde{c}	=	integrated normalized concentration

CFC	=	chlorofluorocarbon
COP	=	coefficient of performance
C_p°	=	heat capacity in the limit of zero pressure
f	=	equivalent substance reducing ratio(defined by Eq. 4)
GWP	=	global warming potential
GWP ₁₀₀	=	global warming potential for a time horizon of 100 years
b	=	equivalent substance reducing ratio(defined by Eq. 5)
HCFC	=	hydrochlorofluorocarbon
HCFO	=	hydrochlorofluoroolefin
HFC	=	hydrofluorocarbon
HFO	=	hydrofluoroolefin
IR	=	infrared radiation
k_{OH}	=	rate constant for reaction with OH
LFL	=	lower flammability limit
LL/SL	=	liquid-line/suction line
ODP	=	ozone depletion potential
OH	=	hydroxyl radical

ppvb	=	volume concentration in parts in 10 ⁹
p	=	pressure
Q_{vol}	=	volumetric heating or cooling capacity
R	=	molar gas constant
RE	=	radiative efficiency
RMSD	=	root mean square deviation
t	=	time
T	=	temperature
TH	=	time horizon for GWP
UV	=	ultraviolet radiation
Z	=	compressibility factor (Eq. 6)
α_1, α_2	=	coefficients in Eq. 9
β_1, β_2	=	coefficients in Eq. 10
γ	=	coefficient in Eq. 13
ΔH_{comb}	=	heat of combustion
θ	=	shape factor (defined by Eq. 7)
ρ	=	density
τ	=	atmospheric lifetime
ϕ	=	shape factor (defined by Eq. 8)
ω	=	acentric factor (defined by Eq. 11)

Subscripts

CO ₂	=	carbon dioxide (reference fluid)	j	=	fluid of interest
cond	=	condenser	ref	=	reference fluid
evap	=	evaporator			

Superscripts

crit	=	critical point value	r	=	reduced quantity (defined in Eq. 12)
0	=	ideal-gas state	sat	=	saturation state

REFERENCES

- ASHRAE. 2010a. ANSI/ASHRAE Standard 34-2010. Designation and safety classification of refrigerants. Atlanta: American Society of Heating, Refrigerating, and Air-Conditioning Engineers, Inc.
- ASHRAE. 2010b. ANSI/ASHRAE Standard 15-2010. Safety standard for refrigeration systems. Atlanta: American Society of Heating, Refrigerating, and Air-Conditioning Engineers, Inc.
- Bivens, D. B.; Minor, B. H. 1998. Fluoroethers and other next generation fluids. *Int. J. Refrig.*, 21, 567-576.
- Bolton, W.; Wang, Y.; Thiessen, P. A.; Bryant, S. H. 2008. PubChem: Integrated platform of small molecules and biological activities; vol. 4, chap. 12. In *Annual Reports in Computational Chemistry*, American Chemical Society: Washington, DC.
- Brown, J.S. 2009. HFO's: New, low global warming potential refrigerants. *ASHRAE J.*, 51(8):22-29.
- Brown, J.S., 2007. Preliminary selection of R-114 replacement refrigerants using fundamental thermodynamic parameters (RP-1308). *HVAC and R Res.* 13, 697-709.
- Brown, J.S., Domanski, P.A., and Lemmon, E.W. 2012. NIST Standard Reference Database 49, CYCLE_D: NIST Vapor Compression Cycle Design Program, version 5.0, National Institute of Standards and Technology.
- Directive 2006/40/EC of The European Parliament & of the Council of 17 May 2006 Relating to Emissions from Air-Conditioning Systems in Motor Vehicles & Amending Council Directive 70/156/EC. *Official Journal of the European Union*, 49(L 161):12-18.

- DIPPR. 2011. *Evaluated Standard Thermophysical Property Values, 801*. Design Institute for Physical Properties, American Institute of Chemical Engineers: New York.
- Domanski, P. A.; Didion, D. A.; Doyle, J. P. 1994. Evaluation of suction-line/liquid-line heat exchange in the refrigeration cycle. *Int. J. Refrig.*, 17, 487-493.
- Fekete, Z. A.; Hoffmann, E. A.; Körtvélyesi, B. 2007. Harmonic vibrational frequency scaling factors for the new NDDO Hamiltonians: RM1 and PM6. *Molecular Physics* 105, (19-22), 2597-2605.
- Goldberg, D. E. 1989. *Genetic Algorithms in Search, Optimization, and Machine Learning*. Addison Wesley Longman, Inc.: Reading, MA.
- Houghton, J.; Meira Filho, L.; Callander, B.; Harris, N.; Kattenbuerg, A.; Maskell, K. 1996. *Climate Change 1995: The Science of Climate Change* Cambridge University Press: New York.
- Huber, M.L. and Ely, J.F. 1994. A predictive extended corresponding states model for pure and mixed refrigerants including an equation of state for R-134a. *Int. J. Refrig.*, 17, 18-31.
- Kazakov, A.; Muzny, C. D.; Diky, V.; Chirico, R. D.; Frenkel, M. 2010. Predictive correlations based on large experimental datasets: Critical constants for pure compounds. *Fluid Phase Equilib.*, 298, 131-142.
- Kazakov, A.; McLinden, M. O.; Frenkel, M. 2012. Computational design of new refrigerant fluids based on environmental, safety, and thermodynamic characteristics. *Ind. Eng. Chem. Res.* (accepted for publication) doi 10.1021/ie3016126.
- Klamt, A. 1993. Estimation of gas-phase hydroxyl radical rate constants of organic compounds from molecular orbital calculations. *Chemosphere* 32, 717-726.
- Kwok, E. S. C.; Atkinson, R. 1995. Estimation of hydroxyl radical reaction rate constants for gas-phase organic compounds using a structure-reactivity relationship: An update. *Atmos. Environ.*, 29, 1685-1695.
- Lagorce, D.; Sperandio, O.; Galons, H.; Miteva, M. A.; Villoutreix, B. D. 2008. FAF-Drugs2: Free ADME/tox filtering tool to assist drug discovery and chemical biology projects. *BMC Bioinformatics* 9, 396.
- Lemmon, E. W.; Huber, M. L.; McLinden, M. O. 2010 *NIST Standard Reference Database 23, NIST Reference Fluid Thermodynamic and Transport Properties—REFPROP, version 9.0*. Standard Reference Data Program, National Institute of Standards and Technology: Gaithersburg, MD.
- Mascarelli, A. L. 2010. A bright future for the Montreal Protocol. *Environ. Sci. Technol.* 44, 1518-1520.
- McLinden, M.O. 1990. Optimum refrigerants for non-ideal cycles: An analysis employing corresponding states. *USNC/IIR-Purdue Refrigeration Conference and ASHRAE-Purdue CFC Conference*, West Lafayette, Indiana, Retrieved June 22, 2012, from <http://docs.lib.purdue.edu/cgi/viewcontent.cgi?article=1088&context=iracc>.
- McLinden, M.O., Didion, D.A. 1987. CFCs: Quest for Alternatives. *ASHRAE J.* 29(12), 32-42
- McQuarrie, D. A. 1976. *Statistical Mechanics*. Harper and Row: New York.
- Midgley, T. 1937. From the periodic table to production. *Industrial and Engineering Chemistry* 29: 241-244
- Montzka, S. A.; Spivakovsky, C. M.; Butler, J. H.; Elkins, J. W.; Lock, L. T.; Mondeel, D. J. 2000. New observational constraints for atmospheric hydroxyl on global and hemispheric scales. *Science*, 288, 500-503.
- Pinnock, S.; Hurley, M. D.; Shine, K. P.; Wallington, T. J.; Smyth, T. J. 1995. Radiative forcing of climate by hydrochlorofluorocarbons and hydrofluorocarbons. *J. Geophys. Res.*, 100, 23227-23238.
- Seybold, L.; Hill, W.; Robin, J.-J. 2011. Internal heat exchanger system integration for R1234yf refrigerant. *SAE Int. J. Mater. Manuf.* 4, 181-194.
- U.S. Department of State. 2009. North American amendment proposal to phase down use of HFCs under the Montreal Protocol. Retrieved June 22, 2012, from www.state.gov/r/pa/prs/ps/2011/05/162930.htm; and retrieved May 31, 2012, from http://ozone.unep.org/Meeting_Documents/mop/21mop/MOP-21-3-Add-1E.pdf
- U.S. Environmental Protection Agency. 2010 *The Atmospheric Oxidation Program for Microsoft Windows (AOPWIN) v1.92a*.
- U.S. Environmental Protection Agency. 2012. Acceptable Substitutes for CFC-114 and CFC-11 in Chillers and Other Refrigerants. Retrieved September 5, 2012 from <http://www.epa.gov/ozone/snap/refrigerants/lists/114cent.html>.
- Vidal, M.; Rogers, W.; Holste, J.; Mannan, M. 2004. A review of estimation methods for flash points and flammability limits. *Process Saf. Prog.*, 23, 47-55.
- Wojtusiak, J.; Michalski, R. S. 2006. The LEM3 implementation of learnable evolution model and its testing on complex function optimization problems. *Genetic and Evolutionary Computation Conference, GECCO*, Seattle, WA.
- Wojtusiak, J. 2011. EOS-EVOL optimization tool. Private communication. George Mason University, Fairfax, VA.